An Efficient 2D Rough Surface Scattering Analysis Using Strong Harmonics Extraction and the Kirchhoff Approach

A. Torabi and A. A. Shishegar

Department of Electrical Engineering,
Sharif University of Technology, Tehran, Iran
torabi@ee.sharif.edu, shishegar@sharif.edu

Abstract ― An efficient method for scattering analysis from slightly rough surfaces is introduced. This method can be used in ray tracing algorithm where the computational efficiency is important due to the complexity and size of problems. In this method, the Kirchhoff approach is used for a periodic extension of the finite surface, which is approximated by strong harmonics of its Fourier series. Typical asphalt surfaces are analyzed by this method in millimeter-wave band and validated with the method of moments. The dominant scattering angles and ray widths of the scattered field can be easily used in ray tracing algorithm. The computation time and accuracy of results show that this method can be used for rough surface scattering analysis in ray tracing algorithm efficiently.

Index Terms - Electromagnetic scattering by rough surfaces, Fourier series, Kirchhoff approach, method of moments, and Ray tracing.

I. INTRODUCTION

The problem of scattering from rough surfaces has been the subject of intensive researches over the past decades. Scattering consideration from these surfaces in ray tracing algorithm is another challenging problem. The existent empirical models have no enough accuracy [1, 2]. Furthermore, accurate numerical analysis of scattering from these surfaces [3, 4], is not practical for use in ray tracing algorithm due to the computational costs.

The Kirchhoff approach is a classical scattering analysis solution based on the tangent plane approximation and is valid for surfaces with large radii of curvature [5]. This method has an analytical closed-form solution for finite length of a periodic rough surface (finite periodic surface, like $f(x)=\cos(\alpha x)$ for $-L \le x \le L$, $L=\pi m/\alpha$, $m=2, 3, \ldots$) [6].

In this paper a novel method is introduced for plane wave scattering analysis from slightly rough surfaces using strong harmonics extraction and the Kirchhoff. The rough surfaces are assumed to be in the validity region of the Kirchhoff approach. The Kirchhoff approach is utilized for the finite periodic surface, which is composed of different harmonics. First, a given rough surface is considered as a period of a periodic surface and is represented by its Fourier series. Then the surface is approximated by its strong harmonics. At last, the Kirchhoff approach is used for computation of scattering from the approximated surface. An important parameter is the number of extracted harmonics, N. Small N makes a big deviation from original rough surface when big N increases the computation time. Typical asphalt surfaces in millimeter-wave band are simulated using this method. Results are compared to the method of moments' results for plane wave incidence using the resistive sheet tapering method **[7]**. It is shown that extracting enough harmonics leads to a good global conformity to the accurate answer. Closed-form scattering coefficient can efficiently represent the scattered field as a sum of rays, directed to dominant scattering angles. This method can be easily integrated to ray tracing algorithm.

In the next section, Kirchhoff approach for finite periodic surfaces is presented. Section III is about the strong harmonics extraction. In section

Submitted On: April 14, 2013
Accepted On: March 8, 2014

IV, numerical results of the scattering computation for slightly rough Gaussian surfaces are shown. The paper is concluded in section V.

II. KIRCHHOFF APPROACH FOR PERIODIC SURFACES

Consider a one dimensional rough surface $z = f(x)$ of length $2L$ as shown in Fig. 1. The normalized scattering coefficient for a plane wave scattering from a rough surface is defined by,

$$\rho = \frac{E_s}{E_{s_0}}, \tag{1}$$

where E_s is the scattered field and E_{s_0} is the field reflected in the specular direction ($\theta_s = \theta_i$) by the same size smooth conducting plane under the same angle of incident.

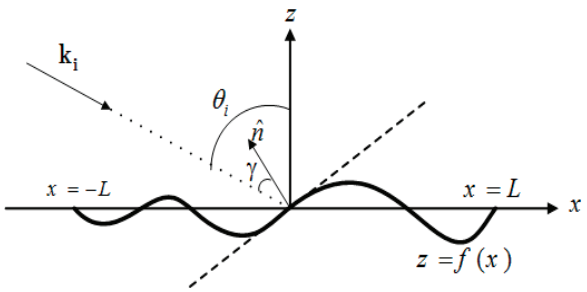

Fig. 1. Rough surface and tangent plane approximation.

For a perfect electric conductor surface, equation (1) has a closed analytic form by using the Kirchhoff approach [6],

$$\rho^{\pm}(\theta_i,\theta_s) = \pm F(\theta_i,\theta_s)\frac{1}{2L}\int_{-L}^{L} e^{j\mathbf{v}.\mathbf{r}(x)}dx + \frac{e^{\pm}(L)}{2L}, \tag{2}$$

$$F(\theta_i,\theta_s) = \sec\theta_i \frac{1+\cos(\theta_i+\theta_s)}{\cos\theta_i+\cos\theta_s}, \tag{3}$$

$$e^{\pm}(L) = \frac{j\sec\theta_i \sin\theta^{\pm} e^{j\mathbf{v}.\mathbf{r}(x)}}{k(\cos\theta_i+\cos\theta_s)}\Bigg|_{-L}^{L} \tag{4}$$

$$\theta^{+} = \theta_s \quad \theta^{-} = \theta_i,$$

where + and − denote TE and TM incident, respectively, θ_i, θ_s are incident and scattering angles, k is the wave number, $\mathbf{r(x)} = x\hat{x} + f(x)\hat{z}$ and $\mathbf{v}$ is the difference of incident and scattered wave vectors,

$$\mathbf{v} = v_x\hat{x} + v_z\hat{z} = \mathbf{k_i} - \mathbf{k_s}. \tag{5}$$

The second term in equation (2) is the edge effect. It is negligible for $L >> \lambda$ if $f(L) = f(-L) = 0$ [6]. Now consider a periodic surface with period Λ (i.e., $f(x) = f(x+\Lambda)$). So in equation (2) exponential term $e^{j\mathbf{v}.\mathbf{r}(x)}$ will be periodic,

$$v_x\Lambda = 2\pi m\ ,\ m = 1,\ 2,\ 3,\ \ldots\ . \tag{6}$$

It is shown that in [6],

$$\sin\theta_{sm} = \sin\theta_i + m\frac{\lambda}{\Lambda};\ (m = 0,\ \pm 1,\ \ldots). \tag{7}$$

Equation (7) is the well-known grating equation. For distinct θ_i, equation (7) is satisfied by specific m. First consider $L = (n+n_1)\Lambda$, where n is an integer and $0 \le n_1 < 1$. Then, after some simplifications,

$$\rho^{\pm}(\theta_i,\theta_{sm}) = \pm\frac{F(\theta_i,\theta_{sm})}{2L}\frac{1}{\Lambda}\int_0^{\Lambda} e^{j\mathbf{v}.\mathbf{r}(x)}dx + \frac{C(n_1)}{2L}, \tag{8}$$

$$C(n_1) = \pm F(\theta_i,\theta_{sm})\left[\int_{-n_1\Lambda}^{n_1\Lambda} e^{j\mathbf{v}.\mathbf{r}}dx - 2n_1\int_0^{\Lambda} e^{j\mathbf{v}.\mathbf{r}}dx\right] + e^{\pm}(2\pi m n_1/v_x). \tag{9}$$

The symbol $C(n_1)$ represents the edge effect. For each θ_{sm} there is a lobe around it with half-width of [6],

$$\Delta\theta_{sm} \approx \frac{\lambda}{2L}\sec(\theta_{sm}). \tag{10}$$

Consider a sinusoidal surface, i.e., $f(x) = h\cos Kx$, where $K = 2\pi/\Lambda$ is the phase constant of the surface. Equation (8) yields to [6],

$$\rho^{\pm}(\theta_i,\theta_{sm}) \approx \pm j^m F(\theta_i,\theta_{sm})J_m(s), \tag{11}$$

$$s = v_z h = -kh(\cos\theta_i + \cos\theta_{sm}), \tag{12}$$

where θ_{sm} is given by the grating equation (7) for each valid m, and $J_m(s)$ is the m-th order of the first kind Bessel function. This solution leads to some scattering lobes, directed to θ_{sm} angles with half-width of $\Delta\theta_{sm}$.

III. STRONG HARMONICS EXTRACTION FOR RANDOMLY ROUGH SURFACES

In the first step of strong harmonics extraction analysis, the rough surface (Fig. 1), is considered as a period of a periodic function (with period of $\Lambda = 2L$) represented by its Fourier series. This series is a summation of $\alpha_n \cos(nKx)$ and $\beta_n \sin(nKx)$ terms. Consider the first harmonic coefficient of cosine part, α_1 and $N-1$ strongest coefficients among other α_n s and β_n s. The selected harmonics are sorted based on their incremental indices. Now the sorted coefficients are saved in new variables a_n and b_n and their indices are saved in new variables c_n and d_n, respectively. So the approximated rough surface is

$$\tilde{f}(x) = a_1 \cos(Kx) + \sum_{m=2}^{N_1} a_m \cos(c_m Kx) + \sum_{m=1}^{N_2} b_m \sin(d_m Kx),$$

$$a_m = \frac{2}{L}\int_{-L}^{L} f(x)\cos(\frac{n\pi}{L})\,dx$$

$$b_m = \frac{2}{L}\int_{-L}^{L} f(x)\sin(\frac{n\pi}{L})\,dx$$

$$a_1 = \alpha_1, \quad K = \frac{2\pi}{\Lambda} = \frac{\pi}{L}, \quad N_1 + N_2 = N. \quad (13)$$

a_n and b_n can be computed numerically. To drive the closed analytical form of the normalized scattering coefficient, the first harmonic ($\cos(Kx)$) is always kept. It must be notified that equation (13) is an approximation of $z = f(x)$ on its domain, i.e., from $-L$ to L ($\Lambda = 2L$). Applying equation (8) to the approximated surface, equation (13), ignoring the edge effect and after some simplifications, the normalized scattering coefficient becomes (see appendix A),

$$\rho(\theta_i, \theta_{sm}) \approx \pm F_2(\theta_i, \theta_{sm}) \times \sum_{q_1=-\infty}^{\infty} \sum_{q_2=-\infty}^{\infty} \dots \sum_{q_{N_1-1}=-\infty}^{\infty} \sum_{p_1=-\infty}^{\infty} \sum_{p_2=-\infty}^{\infty} \dots \sum_{p_{N_2}=-\infty}^{\infty} \Big[J_{q_1}(s_{N_1}) \times J_{q_2}(s_{N_1-1}) \dots \times J_{q_{N_1-1}}(s_2) J_{p_1}(w_{N_2}) J_{p_2}(w_{N_2-1}) \dots J_{p_{N_2}}(w_1) \times J_T(s_1) \times j^D \Big], \quad (14)$$

where

$$s_i = v_z a_i, \; i = 1, 2, 3, \dots, N_1, \quad (15)$$

$$w_i = v_z b_i, \; i = 1, 2, 3, \dots, N_2, \quad (16)$$

$$T = m + \sum_{i=1}^{N_1-1} c_{N_1-i+1} q_i + \sum_{i=1}^{N_2} d_{N_2-i+1} p_i, \quad (17)$$

$$D = m + \sum_{i=1}^{N_1-1} q_i + \sum_{i=1}^{N_1-1} c_{N_1-i+1} q_i + \sum_{i=1}^{N_2} d_{N_2-i+1} p_i, \quad (18)$$

where v_z is the $\hat{z}$-component of $\mathbf{v}$, and m is defined by grating equation (7). Equation (14) is an $(N-1)$-dimensional series. The Bessel function has intensive decreasing form as its order increases. So the infinite summations of equation (14) can be replaced by the terms of q_i and p_i in $[-M, M]$.

Equation (14) is the closed-form normalized scattering coefficient for the slightly rough perfect conductor surfaces. To use this method in ray tracing algorithm, the scattered field can be assumed as some rays (exactly m rays, where m is given by equation (7)) directed to θ_{sm} with the normalized amplitude given by truncated form of equation (14). So one can choose the dominant angles using an appropriate amplitude threshold and import them in ray tracing algorithm. In the next section we validate this formulation and explain about different parameters of it.

IV. VALIDATION AND RESULTS

To validate the above method, we consider the asphalt surface with roughness parameters of Table I. Both types of considered asphalt surfaces, satisfy the Kirchhoff approach condition for millimeter wave band ($\lambda = 5mm$ and $\lambda = 10mm$) [5]. The formula in equation (14) is for perfect conductor surface, but in millimeter-wave band, one can replace the lossy dielectric surface with perfect conductor as a good approximation because of the small penetration depth [10]. These two Gaussian random surfaces are generated numerically by spectral approach [3]. Without loss of generality, an even extension of each surface is generated. So the coefficients b_m are zero. Extraction of the first harmonic and the strong $N-1$ harmonics is the next step. Table II shows this process and their prominent extracted Fourier

series coefficients. Criterion for approximation is $\Delta \le 20\%$, where

$$\Delta = \frac{\int_{-L}^{L} \left| f(x) - \tilde{f}(x) \right| dx}{\int_{-L}^{L} \left| f(x) \right| dx}, \qquad (19)$$

while $f(x)$ is the original rough surface and $\tilde{f}(x)$ is the approximated surface given by equation (13). An efficient approach to find the dominant coefficients of Fourier series is defining an internal error criterion, which computes the change of Δ in each step of finding a_i (b_i). Then if the evaluated $a_i\,(b_i)$ satisfy this internal criterion, it means that the derived Fourier coefficient is dominant and it could be kept. Otherwise, that would be ignored. The second step is the calculation of θ_{sm}. Valid θ_{sm} and m could be found by equation (7). By replacing θ_{sm} in equation (14), approximated $\rho(\theta_i, \theta_{sm})$ could be solved for each θ_{sm}. For each θ_{sm} scattering angle, there is a lobe with half-width that is given by equation (10). For validation, the method of moments (MOM) is used [3, 9].

Table I: Asphalt surface parameters [8].

Asphalt surface type	σ(mm)	l_c(mm)
Type1(slightly rough asphalt)	0.36	≈ 5.2
Type2 (very rough asphalt)	0.7	≈ 5

Table II: Strong harmonics extracted for two asphalt surface for $\Delta \le 20\%$.

Asphalt surface type	N	$\{a_n\}$	Δ
Type1	4	$\{a_1, a_3, a_4, a_8\}$	18.22%
Type2	5	$\{a_1, a_3, a_8, a_{10}, a_{17}\}$	14.83%

Because in the harmonics extraction method the incident wave is supposed to be a uniform plane wave and the edge effect is ignored, so for validating the results with MOM, uniform plane wave incident must be considered in numerical analysis too. For this goal, resistive sheet tapering method is used [7]. In this method, a relatively small portion of the sample surface is used to suppress the edge currents. Figures 2 and 3 show the normalized scattering coefficient for these two types of asphalt surfaces in two wavelengths ($\lambda = 5mm$ and $10mm$, respectively). θ_i, the incident angle is 30° and $M = 8$ is chosen. It can be seen that for the rougher surface (type 2), scattering in non-specular direction becomes more prominent than the other (type 1). The deviation between the harmonic extraction analysis and MOM results of Figs. 2 and 3 is due to some approximation in deriving the relation in equation (14). But the global behavior of the scattered field pattern has an acceptable conforming to MOM.

The main reason for deviation of the results with MOM is related to this fact that the MOM reported results are related to scattering computation of large number of realizations for desired Gaussian rough surface, which are averaged. Therefore, our method has this ability to follow this average behavior acceptably. One of the error sources is the truncation of the series in equation (14) (value of M) and the other is the number of the extracted harmonics (N in equation (13)). Consider the asphalt surface type 1. Now consider three different scattering angles in Fig. 2 (a); $\theta_s = 30^\circ$, $\theta_s = 11.53^\circ$, $\theta_s = -30^\circ$. Positive angles are in clockwise. For these angles, normalized scattering coefficient for $M = 6$, 8, 10, and 12 are calculated and shown along with the MOM results in Table III. Due to small magnitude of the high order Bessel functions, ignoring the high values of M gives acceptable results. We can see that the differences between $M = 6$ and $M = 8$ are negligible. The results for $M = 10$ and $M = 12$ are the same. It can be concluded that the truncation of series in equation (14) does not cause a big change in the results. Another important error source is the number of the extracted harmonics. Higher N, increases the order of series in equation (14) and consequently the time of the computation process would increase severely.

Table III: $\rho(30^\circ, \theta_{sm})$ for different values of M (truncation effect in series of equation (14)).

M	$\theta_{sm} = 30^\circ$ (MOM : 0.9812)	$\theta_{sm} = 11.53^\circ$ (MOM : 0.0950)	$\theta_{sm} = -30^\circ$ (MOM : 0.0830)
6	0.9655	0.1000	0.1033
8	0.9698	0.1001	0.1044
10	0.9700	0.1002	0.1074
12	0.9700	0.1002	0.1074

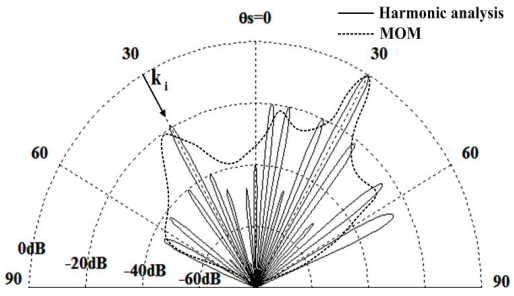

(a)

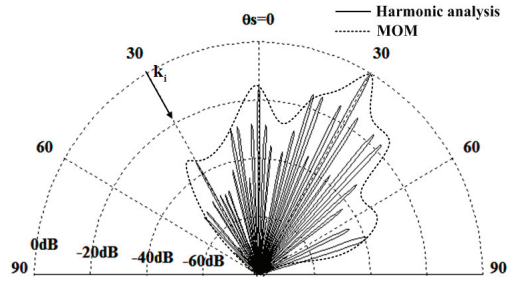

(b)

Fig. 2. Strong harmonics extraction analysis for asphalt type 1, L = 5 *cm* (a) $\theta_i = 30^o$, λ = 10 *mm* and (b) $\theta_i = 30^o$, λ = 5 *mm*, mean time for MOM is 8 min while for the relation in equation (19) is less than 5 sec.

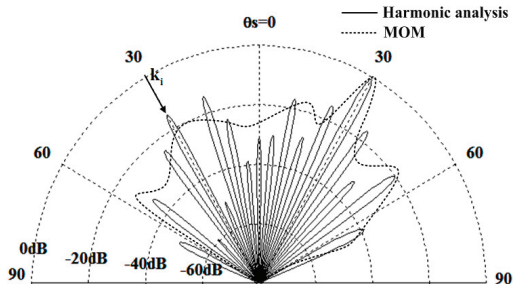

(a)

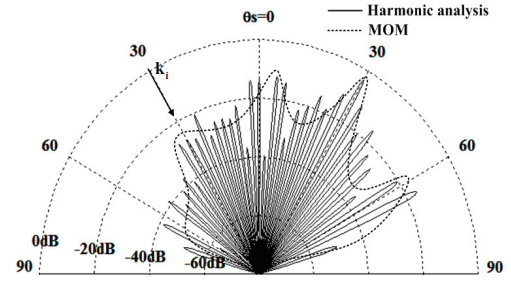

(b)

Fig. 3. Strong harmonics extraction analysis for asphalt type 2, L = 5 *cm* (a) $\theta_i = 30^o$, λ = 10 *mm* and (b) $\theta_i = 30^o$, λ = 5 *mm*, mean time for MoM is 8 min while for the relation in equation (19) is less than 5 sec.

Figure 4 represents the results for different number of extracted harmonics, N = 3, 4, 5, and 7, for rough surface of type 1 asphalt. For small N, (N = 3), a big error ($\Delta = 30\%$) in the approximation of the original surface resulted a bad conformity to the MOM method. It is obvious that by increasing N, a better answer is achievable (Fig. 4 (b), (c), (d)). By extracting more harmonics to some extent, the accuracy of the method will improve. But extracting more harmonics doesn't make notable change in the global form of the scattering pattern. So it can be seen that approximation with $\Delta \leq 20\%$ gives acceptable converged results. For two surfaces above, 4-5 strong harmonics must be extracted for $\Delta \leq 20\%$ (Table II). Our simulations show that decreasing Δ from 20% to 10% results 2% change in $\rho(\theta_i, \theta_{sm})$. One can define a threshold for the normalized scattering coefficients to select the dominant scattering angles. These angles show proper rays for ray tracing algorithm. The results are shown in Table IV for a -30dB threshold. Consequently, 6 rays is extracted and listed in Table IV. Apart from the specular direction with dominant amplitude, there are 5 rays, which are above the threshold (-30 dB). The ray width of each ray is also indicated in the following table.

Table IV: Selected scattering angles and the ray widths for threshold of -30dB.

Selected θ_{sm}	**53.13°**	**36.86°**	**30°**	**23.57°**	**11.53°**	**-30°**
$\rho(30^\circ, \theta_{sm})$	-22.2*dB*	-20.8*dB*	-0.13*dB*	-19.5*dB*	-20.2*dB*	-21.0*dB*
$\Delta\theta_{sm}$	9.568°	7.162°	6.589°	6.251°	5.847°	6.589°

V. CONCLUSION

A new method for rough surface scattering analysis for ray tracing algorithm is introduced. This method is enough accurate, computationally efficient and can be integrated well with the ray tracing algorithm. A rough surface is extended to a periodic rough surface first. Then, the surface is approximated by its strong harmonics of the Fourier series. The Kirchhoff approach is used for the approximated surface over a period, i.e., the length of the original rough surface. The scattering pattern in this method can be assumed as a sum of different rays at different angles, called the scattering angles. Using a proper threshold, the dominant rays can be chosen to be used in ray

tracing algorithm. The numerical results show a good global conformity to the results of the method of moments. The method is computationally efficient and can be easily integrated to the ray tracing algorithm.

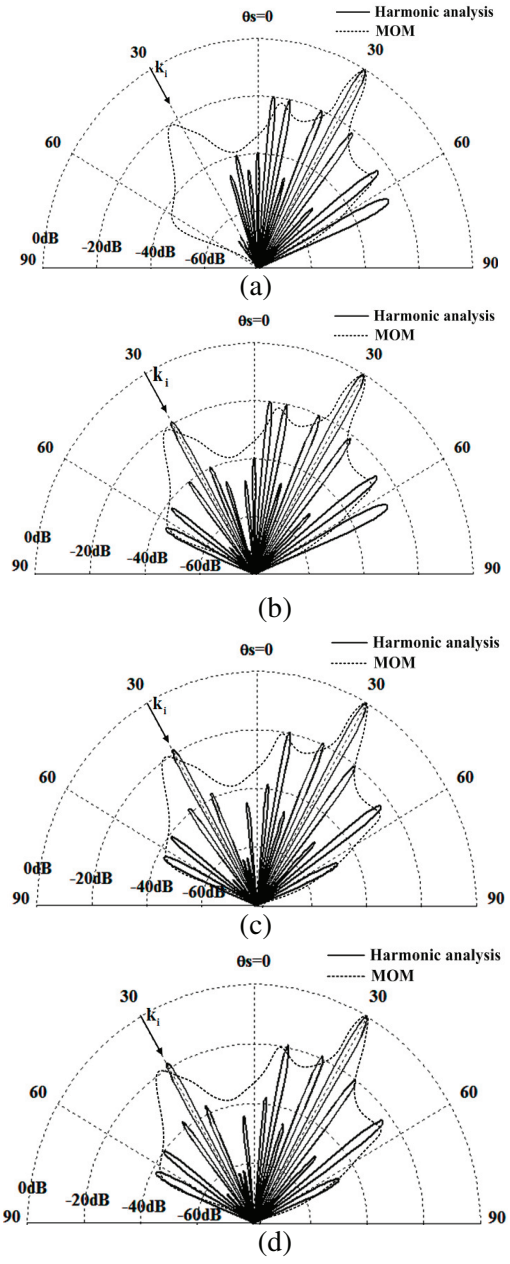

Fig. 4. Strong harmonics extraction analysis for asphalt type 1, $L = 5\ cm$ (a) $N = 3(\Delta = 30\%)$, (b) $N = 4(18.22\%)$, (c) $N = 5(\Delta = 10.32\%)$, and (d) $N = 7(\Delta = 8.03\%)$, mean time for MoM is 8 min while for the relation in equation (19) is 0.2, 0.9, 1.3, and 4.5 sec for $N = 3$, 4, 5, and 7, respectively.

ACKNOWLEDGMENTS

The authors wish to thank Iran Telecommunication Research Center (ITRC) for supporting this research.

APPENDIX A

By replacing the approximated rough surface of equation (13) into equation (8) and ignoring the edge effect,

$$\frac{1}{\Lambda}\int_0^{\Lambda} e^{j\mathbf{v}.\mathbf{r}}dx = \frac{1}{\Lambda}\int_0^{\Lambda} e^{j\left\{\mathbf{v}_x x + v_z\left(a_1\cos(Kx)+\sum_{m=2}^{N_1}a_m\cos(c_mKx)+\sum_{m=2}^{N_2}b_m\sin(d_mKx)\right)\right\}}dx \tag{20}$$

we also have in [11],

$$e^{jx\cos\theta} = \sum_{m=-\infty}^{\infty} j^m J_m(x) e^{jm\theta}, \tag{21}$$

$$e^{jx\sin\theta} = \sum_{m=-\infty}^{\infty} J_m(x) e^{jm\theta}. \tag{22}$$

Using equations (21) and (22) in equation (20) and by replacing $Kx = t$, equation (20) is changed to,

$$\sum_{q_1=-\infty}^{\infty}\sum_{q_2=-\infty}^{\infty}\cdots\sum_{q_{N_1-1}=-\infty}^{\infty}\sum_{p_1=-\infty}^{\infty}\sum_{p_2=-\infty}^{\infty}\cdots\sum_{p_{N_2}=-\infty}^{\infty}$$
$$\left[J_{q_1}(s_{N_1})J_{q_2}(s_{N_1-1})\ldots J_{q_{N_1-1}}(s_2)\times\right.$$
$$\left.J_{p_1}(w_{N_2})J_{p_2}(w_{N_2-1})\ldots J_{p_{N_2}}(w_1)\right]\times$$
$$\int_0^{2\pi} e^{j\left(\left[m+\sum_{i=1}^{N_1-1}c_{N_1-i+1}q_i+\sum_{i=1}^{N_2}d_{N_2-i+1}p_i\right]t+s_1\cos(t)\right)}dt \tag{23}$$

where s_i and w_i are defined in equations (15) and (16). Then by using another Bessel identity in [11] yield,

$$\frac{1}{2\pi}\int_0^{2\pi} e^{jmt+jv_z h\cos t}dt = j^m J_m(v_z h), \tag{24}$$

in equation (23), relation (14) will be concluded.

REFERENCES

[1] ITU-R-P.1410, "Propagation data and prediction methods required for the design of terrestrial broadband radio access systems operating in a frequency range from 3 to 60 GHz," 2007.

[2] W. Ament, "Toward a theory of reflection by a rough surface," *IRE Proc.*, vol. 41, no. 1, pp. 142-146, 1953.

[3] J. Kong and L. Tsang, *Scattering of Electromagnetic Waves (Numerical Simulations)*, vol. 2, John Wiley & Sons, 2001.
[4] J. Li, L. X. Guo, and H. Zeng, "FDTD investigation on electromagnetic scattering from two-dimensional layered rough surfaces," *Applied Computational Electromagnetics Society (ACES) Journal*, vol. 25, no. 5, pp. 450-457, May 2010.
[5] A. Fung, *Microwave Scattering and Emission Models and Their Applications*, Artech House Inc., 1994.
[6] P. Bekkmann and A. Spizzicino, *The Scattering of Electromagnetic Waves from Rough Surface*, Artech House, 1987.
[7] Y. Oh and K. Sarabandi, "Improved numerical simulation of electromagnetic wave scattering from perfectly conducting random surfaces," *IEE Proceedings: Microw. Antennas Propag.*, vol. 144, no. 4, pp. 256-260, 1997.
[8] L. Ibos, et al., "Infrared emissivity measurement device: principle and applications," *Meas. Sci. Technol.*, vol. 17, pp. 2950-2956, 2006.
[9] R. Harrington, *Field Computation by Moment Methods*, New York: Macmillan, 1968.
[10] T. Peters, et al., "Simulation of two-dimensional dielectric structures with resistive sheets," *The University of Michigan, Radiation Laboratory*, no. 389055-1-F, 1986.
[11] M. Abramowitz and I. Stegun, *Handbook of Mathematical Functions*, Washington DC, 1970.